

GHOSTING-FREE MULTI-EXPOSURE IMAGE FUSION IN GRADIENT DOMAIN

K. Ram Prabhakar, R. Venkatesh Babu

Department of Computational and Data Sciences,
Indian Institute of Science,
Bangalore, India.

ABSTRACT

This paper presents an algorithm to produce ghosting-free High Dynamic Range (HDR) image by fusing set of multiple exposed images in gradient domain. Recently proposed Gradient domain based exposure fusion method provides high quality result but the scope of which is limited to static camera without foreground object motion. The presence of moving objects/hand shake produces a set of misaligned images. The result of gradient domain approach on misaligned images suffers from ghosting artifacts. In order to produce better HDR image without image registration, we propose to create an aligned image set from input image set by photometric calibration. The gradient of aligned image set is then used to reconstruct the fused final image. The proposed algorithm tested on several publicly available dynamic image sets shows that resultant HDR image is ghosting-free and well exposed. Additionally, the proposed method is fast and thus can be used in consumer appliances such as mobile phones, portable devices with digital cameras.

Index Terms— Exposure Fusion, High Dynamic Range Imaging, Deghosting, Brightness transfer function

1. INTRODUCTION

The range of brightness in real world scene is huge, which most often cannot be captured completely using existing camera sensors. Due to this limitation, images of sunlit scenes and scenes with varying exposure end up being too bright or too dark in some regions. A widely followed approach to get better dynamic range is to use exposure fusion, in which, a series of Low Dynamic Range (LDR) images with varying exposure are combined to form a single HDR image containing better illumination for all regions.

Cameras with any kind of internal exposure meter usually feature an exposure compensation setting which is intended to allow the photographer to simply offset the exposure level from the internal meter's estimate of appropriate exposure. This camera setting is usually calibrated in terms of Exposure Value (EV) units, where " EV_{+1} " indicates twice (2^1) as much exposure and " EV_{-1} " means half (2^{-1}) as much exposure compared to EV_0 .

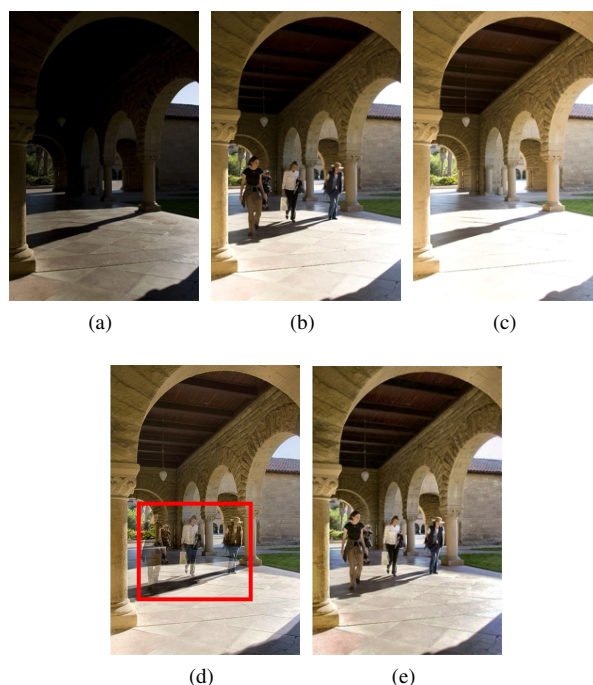


Fig. 1. (a) EV_{-2} : Under exposed image (b) EV_0 (c) EV_2 : Over exposed image (d) Result from Gradient domain fusion approach [1] (e) Result from proposed approach

In several existing fusion approaches, input images are assumed to be aligned. Under that assumption, every pixel is combined using fusion weight, which is determined based on a number of factors, such as contrast, color saturation, and exposure level. The output image is then obtained as a weighted sum of exposure images [2]. Wang *et al.* [3] have used sparsity of input images to perform exposure fusion. In their work, they have combined Sparse Representation of the luminance channel of input images. Mertens *et al.* [4] proposed a method to blend images guided by quality measures like saturation, brightness variation and contrast. Another recently proposed method is Gradient Domain fusion method [1]. The motivation behind this method, is that the human visual system is highly sensitive to changes (gradient) in in-

tensities than absolute value of intensities themselves. This method aims to capture gradient of all regions from differently exposed images and reconstruct final fused image from gradient data by integration. These methods perform well for perfectly aligned sequence. However, the assumption of images being well-aligned limits its potential applicability, as, in many real-world applications, there is no guarantee that the input sequence is perfectly aligned. The result of these approaches on misaligned images suffers from ghosting effect, as shown in Fig. 1(d).

De-ghosting process can also be performed as weighted combination of input multiple exposure images. The disadvantage of such approaches is that, non-object pixels may also get mixed up and corrupt the final fused image, in spite of small weight. A recently proposed method by Sei *et al.* [5], produces a temporary image by transferring color from long exposure image to short exposure image, resulting in well aligned images without the need for image registration. Temporary image and short exposure image are then fused using a weight map that was optimized over local scene contrast and exposure level. Kakarala *et al.* [6] proposed to combine the uniform region of the long-exposure image and the detailed region of the short-exposure image based on Discrete Cosine Transform. This method is well suited for real time applications for scenarios with small object movements. For scenes with large object movement, result obtained suffers from color inconsistencies across the image.

A common approach to remove the artifacts due to the camera motion is to first register the LDR images [7]. Registration becomes difficult as the brightness across the image set varies, since most registration algorithms rely on the brightness constancy assumption. In most scenarios, a normally exposed image is chosen as the reference image and then all the other images are registered to this reference image. However, the image registration step is usually time consuming therefore may not be suitable for real time applications.

In the proposed work, inspired by [5], one of the input images is marked as reference image (R) based on the level of saturation. Then, we form aligned images I' from input images I , where for each source image S in I we build a image that looks as if it was taken at the same time as the reference R, but with the exposure settings of S. The gradient of I' is used to produce final fused image by using gradient domain fusion method.

2. PROPOSED METHOD

2.1. Image alignment

The input image set I has a set of under exposed images (EV_{-m}), normally exposed image (EV_0) and a set of over exposed images (EV_m) (where m denotes exposure calibration in stops). The proposed algorithm selects an image with

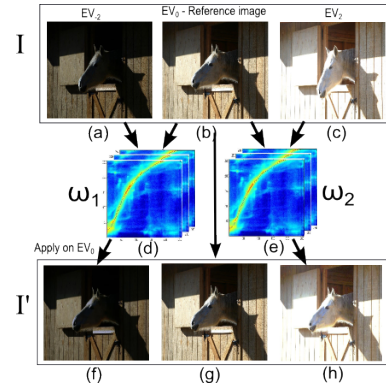


Fig. 2. Input image set, I : (a)-(c). (a) Under exposed image (EV_{-2}). (b) Normally exposed reference image (EV_0). (c) Over exposed image (EV_2). (d) IMF between (a) and (b). (e) IMF between (b) and (c). Aligned image set, I' : (f)-(h). (f) EV_0 after applying ω_1 . (g) Reference image. (h) EV_0 after applying ω_2

fewer saturated regions as reference image, R . In Fig. 2, the normal exposure image (EV_0) is selected as R , as it has few saturated regions as compared to under exposed (EV_{-2}) and over exposed (EV_2) images (For simplification of illustration, the proposed algorithm is applied on 3 input images but can be extended to more input images also). For every other image S in I , we estimate Intensity Mapping Function (IMF), ω between R and S [8].

For each color channel, we estimate IMF by analyzing the joint histogram of pixel values in the two images, also called Comparagram [9]. If (B_1, B_2) are any two pairs of intensities, then the comparagram $J(B_1, B_2)$ is the number of pixels which have intensity values B_1 in first image and B_2 at corresponding point in second image. We see that ω should ideally relate the intensity values between the images, $B_2 = \omega(B_1)$. This function describes how to map intensity values in one image onto the second image. We estimate the IMF from this comparagram by fitting a low-order polynomial to the data.

In Fig. 2, ω_1 is the intensity mapping function estimated between EV_{-2} and EV_0 . Later, ω_1 is applied on EV_0 (R) to obtain the image S' (as shown in Fig. 2(f)). Structurally, S' looks the same as R since ω_1 alters R photometrically but not structurally. But in exposure level, S' looks similar to S . S' is the image obtained if R was taken with camera settings used to get S . The same process is repeated for EV_2 . At the end of this process, we have aligned image set I' , in which all the images are structurally the same but different in exposure levels.

2.2. Gradient domain fusion

The resultant aligned image set I' from previous step is applied as input to this algorithm. The algorithm shown in Fig. 4 summarizes Gradient domain fusion technique [1].

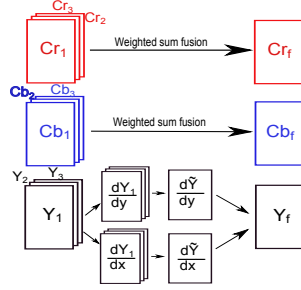


Fig. 3. Overview of Gradient domain fusion. First column: YCbCr components of I' . Last column: Luminance of fused image Y_f , obtained by solving Eqn. (3). Chrominance of fused image, Cb_f and Cr_f , obtained by weighted sum fusion of I chrominance channels using Eqn. (4)

- 1: **procedure** $F = \text{GRADIENT-FUSION}(I')$
- 2: ▷ I' - aligned input image set
- 3: $J \leftarrow \text{RGBTOYCBCR}(I')$
- 4: ▷ J is $(Y_i Cb_i Cr_i), i = 1, \dots, n$ where n is number of input images
- 5: $Y_f \leftarrow \text{FUSEDLUMINANCE}(Y_1, \dots, Y_n)$
- 6: ▷ Obtain fused image luminance from subroutine explained in Fig. 5
- 7: $Cb_f \leftarrow \text{FUSEDCHROMINANCE}(Cb_1, \dots, Cb_n)$
- 8: ▷ Obtain fused image Cb component using Eqn. 4
- 9: $Cr_f \leftarrow \text{FUSEDCHROMINANCE}(Cr_1, \dots, Cr_n)$
- 10: ▷ Obtain fused image Cr component using Eqn. 4
- 11: $F \leftarrow \text{YCBCRTORGB}(Y_f, Cb_f, Cr_f)$
- 12: ▷ F - Final fused HDR image
- 13: **end procedure**

Fig. 4. Summary of gradient domain image fusion algorithm as presented in [1]

The subfunction **FUSEDLUMINANCE** of the algorithm in line 5 of Fig. 4 is explained in following section 2.2.1 and submodule **FUSEDCHROMINANCE** of algorithm in line 7 and 9 of Fig. 4 is explained in the section 2.2.2

2.2.1. Luminance fusion

The gradient of luminance channel $\left[\frac{\partial Y_i}{\partial x} \frac{\partial Y_i}{\partial y} \right]^T$ for every image ($i = 1, \dots, n$) is computed. At every pixel, the gradient across luminance of all input images with maximum gradient magnitude is assigned as gradient of luminance component of fused image, $\left[\frac{\partial \tilde{Y}}{\partial x} \frac{\partial \tilde{Y}}{\partial y} \right]^T$. The relation between luminance of fused image (Y_f) and available gradient data can be expressed as,

$$\nabla Y_f = \begin{bmatrix} \partial \tilde{Y} / \partial x \\ \partial \tilde{Y} / \partial y \end{bmatrix} \quad (1)$$

- 1: **procedure** $Y_f = \text{FUSEDLUMINANCE}(Y_1, \dots, Y_n)$
- 2: ▷ Find gradient of each input luminance channels
- 3: $\left[\frac{\partial Y_i}{\partial x}, \frac{\partial Y_i}{\partial y} \right] \leftarrow \text{COMPUTEGRADIENT}(Y_i)$
- 4: ▷ Use gradient magnitude data to find gradient of fused image luminance as explained in Section 2.2.1
- 5: $\left[\frac{\partial \tilde{Y}}{\partial x}, \frac{\partial \tilde{Y}}{\partial y} \right] \leftarrow \text{MAXPOOLING}\left(\left[\frac{\partial Y_i}{\partial x}, \frac{\partial Y_i}{\partial y} \right] \right)$
- 6: ▷ Apply Poisson solver as explained in Section 2.2.1
- 7: $Y_f \leftarrow \text{POISSONSOLVER}\left(\left[\frac{\partial \tilde{Y}}{\partial x}, \frac{\partial \tilde{Y}}{\partial y} \right] \right)$
- 8: **end procedure**

Fig. 5. The method to find fused image luminance from gradient data [1]

In continuous signal case, integrating Eqn. 1 on both sides will provide required Y_f . But in digital 2D image cases, given gradient data is not integrable (as it violates zero curl condition). Therefore, typical approach to recover images from their gradient data is by using Poisson solvers. Eqn. 1 can be reformulated as minimization problem to estimate Y_f as,

$$Y_f = \min_{Y_f^*} \iint \left[\left(\frac{\partial Y_f^*}{\partial x} - \frac{\partial \tilde{Y}}{\partial x} \right)^2 + \left(\frac{\partial Y_f^*}{\partial y} - \frac{\partial \tilde{Y}}{\partial y} \right)^2 \right] dx dy \quad (2)$$

By differentiating w.r.t x and y and equating to zero, the above equation reduces to,

$$\frac{\partial^2 Y_f}{\partial x^2} + \frac{\partial^2 Y_f}{\partial y^2} = \frac{\partial^2 \tilde{Y}}{\partial x^2} + \frac{\partial^2 \tilde{Y}}{\partial y^2} \quad (3)$$

Eqn. 3 is the Poisson equation and there are various approaches to solve it, given proper boundary conditions. The approach used is based on Haar wavelet decomposition of the image to be reconstructed (detailed derivation is available in Section 3.2 of [10]).

2.2.2. Chrominance fusion

The chrominance components of fused image, Cb_f and Cr_f , can be obtained by weighted sum of input chrominance channel values. If x_1, \dots, x_n denote the Cb (or Cr) channel value at any pixel location for n images, then the fused chrominance value x is obtained as follows,

$$x = \frac{\sum_{i=1}^n x_i (|x_i - \tau|)}{\sum_{i=1}^n |x_i - \tau|} \quad (4)$$

where $\tau = 128$.

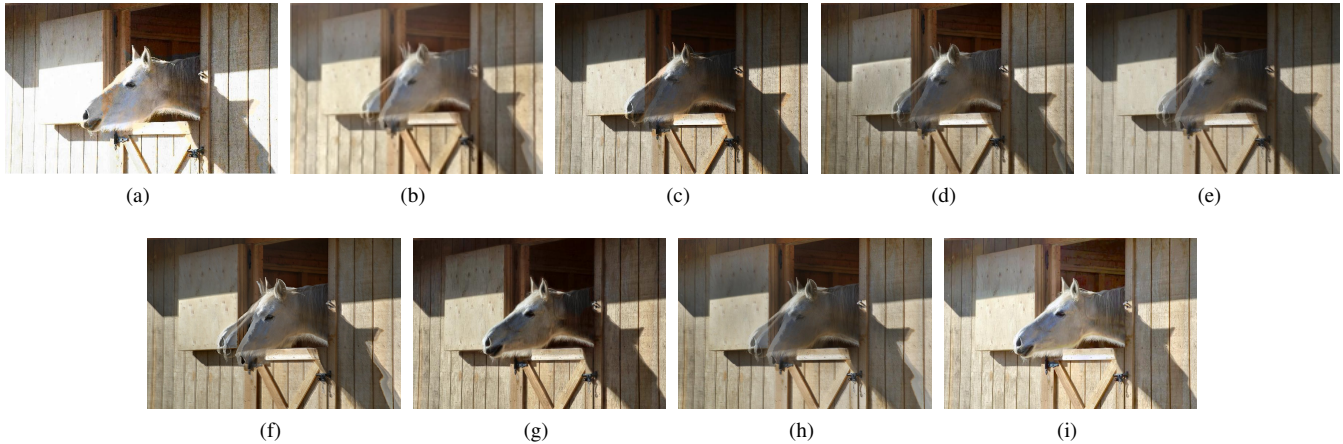


Fig. 6. Fused result for input images from Fig. 2 by (a) Kakarala *et al.* [6] (b) Paul *et al.* [1] (c) Wang *et al.* [3] (d) Vonikakis *et al.* [2] (e) Mertens *et al.* [4] (f) Zhang *et al.* [11] (g) Sen *et al.* [12] (h) Liu *et al.* [13] (i) Proposed approach

Table 1. SSIM performance evaluation of the proposed model against 8 existing models

	set1	set2	set3	set4	set5	set6
Mertens <i>et al.</i> [4]	0.69	0.46	0.87	0.87	0.78	0.62
Wang <i>et al.</i> [3]	0.58	0.67	0.82	0.82	0.78	0.81
Paul <i>et al.</i> [1]	0.86	0.49	0.88	0.79	0.85	0.67
Vonikakis <i>et al.</i> [2]	0.68	0.47	0.89	0.89	0.84	0.61
Kakarala <i>et al.</i> [6]	0.61	0.20	0.27	0.32	0.44	0.37
Zhang <i>et al.</i> [11]	0.74	0.17	0.72	0.82	0.73	0.38
Sen <i>et al.</i> [12]	0.60	0.77	0.84	0.87	0.85	0.81
Liu <i>et al.</i> [13]	0.66	0.49	0.83	0.83	0.80	0.69
Proposed	0.85	0.90	0.90	0.88	0.87	0.94

3. EXPERIMENTAL RESULTS

We compare the performance of the proposed approach with existing 8 state-of-art techniques. Among the 8 techniques, we considered four static scene exposure fusion techniques such as: Gradient domain fusion technique [1], Sparse representation [3], EF [4] and fusion based on illumination estimation [2]. And remaining others are dynamic scene exposure fusion techniques: algorithm proposed by Kakarala *et al.* [6], Sen *et al.* [12], Zhang *et al.* [11] and Liu *et al.* [13]. For the input images shown in Fig. 2, the output of all methods are shown in Fig. 6. The fused result of Kakarala *et al.* is shown in Fig. 6(a), even though the result does not have any ghosting effect, the color distribution is incorrect. This problem occurs, since luminance of boosted short exposure image is merged with chrominance of long exposure image without performing any image alignment step. The proposed approach outperforms static multi-exposure fusion techniques (Fig. 6(b-e)) by producing HDR result that does not have any ghosting effect.

The result generated by Zhang *et al.* [11] and Liu *et al.* [13] approach (shown in Fig. 6 (f) and (h)) introduces ghosting effect due to improper alignment procedures. Figure 6(g) shows the result of using Sen’s algorithm [12]. The under exposed regions (behind the horse) of the image are too dark which have led to loss of details. The same region in Figure 6(i) clearly shows that the proposed algorithm preserves more details. The other image set results are available online¹. We have quantitatively evaluated the performance of algorithms using SSIM score (shown in Table 1). The reference image required to compare is generated using Photomatix [14] software in manual de-ghosting mode. The MATLAB implementation of Kakarala *et al.* method [6] takes about 50 seconds to fuse two images of size $1280 \times 1920 \times 3$. Meanwhile, MATLAB implementation of our method takes about 11 seconds, indicating that our method is roughly 5 times faster than [6]. All experiments are simulated with MATLAB software on a 2.6GHz CPU PC with 4GB RAM and reported timings are averaged over three runs.

4. CONCLUSION

In this paper, we have proposed a method to avoid ghosting effect by gradient domain exposure fusion method without relying on image registration techniques. The proposed method of generating aligned image set from input set by using IMF reduces the computational complexity and time as compared to image registration techniques. Our model estimates fused image from gradient data of aligned image set. The result from our algorithm is compared against several state-of-art static and dynamic multi-exposure fusion techniques and shown to produce high quality ghosting-free HDR result. Further, our method fuses images faster than [6] roughly by a factor of 5, suggesting it’s wide application in consumer devices.

¹http://val.serc.iisc.ernet.in/HDR/icassp2016_hdr/index.html

5. REFERENCES

- [1] Sujoy Paul, Ioana S Sevcenco, and Panajotis Agathoklis, “Multi-exposure and multi-focus image fusion in gradient domain,” submitted for publication. 1, 2, 3, 4
- [2] Vassilios Vonikakis, Odysseas Bouzos, and Ioannis Andreadis, “Multiexposure image fusion based on illumination estimation,” in *Proc. IASTED Int. Conf. on Signal and Image Processing and Applications*, 2011, pp. 135–142. 1, 4
- [3] Jinhua Wang, Hongzhe Liu, and Ning He, “Exposure fusion based on sparse representation using approximate k-svd,” *Neurocomputing*, vol. 135, pp. 145–154, 2014. 1, 4
- [4] Tom Mertens, Jan Kautz, and Frank Van Reeth, “Exposure fusion,” in *Computer Graphics and Applications, 2007. PG’07. 15th Pacific Conference on*. IEEE, 2007, pp. 382–390. 1, 4
- [5] Wei-Rong Sie and Chiou-Ting Hsu, “Alignment-free exposure fusion of image pairs,” in *Proc. ICIP*, 2014. 2
- [6] Ramakrishna Kakarala and Ramya Hebbalaguppe, “A method for fusing a pair of images in the jpeg domain,” *Journal of real-time image processing*, vol. 9, no. 2, pp. 347–357, 2014. 2, 4
- [7] Pei-Ying Lu, Tz-Huan Huang, Meng-Sung Wu, Yi-Ting Cheng, and Yung-Yu Chuang, “High dynamic range image reconstruction from hand-held cameras,” in *Computer Vision and Pattern Recognition, 2009. CVPR 2009. IEEE Conference on*. IEEE, 2009, pp. 509–516. 2
- [8] Michael D Grossberg and Shree K Nayar, “Determining the camera response from images: What is knowable?,” *Pattern Analysis and Machine Intelligence, IEEE Transactions on*, vol. 25, no. 11, pp. 1455–1467, 2003. 2
- [9] Steve Mann, “Comparametric equations with practical applications in quantigraphic image processing,” *Image Processing, IEEE Transactions on*, vol. 9, no. 8, pp. 1389–1406, 2000. 2
- [10] Ioana S Sevcenco, Peter J Hampton, and Panajotis Agathoklis, “A wavelet based method for image reconstruction from gradient data with applications,” *Multidimensional Systems and Signal Processing*, pp. 1–21, 2013. 3
- [11] Wei Zhang and Wai-Kuen Cham, “Reference-guided exposure fusion in dynamic scenes,” *Journal of Visual Communication and Image Representation*, vol. 23, no. 3, pp. 467–475, 2012. 4
- [12] Pradeep Sen, Nima Khademi Kalantari, Maziar Yaesoubi, Soheil Darabi, Dan B Goldman, and Eli Shechtman, “Robust patch-based hdr reconstruction of dynamic scenes.,” *ACM Trans. Graph.*, vol. 3, no. 6, pp. 203, 2012. 4
- [13] Yu Liu and Zengfu Wang, “Dense sift for ghost-free multi-exposure fusion,” *Journal of Visual Communication and Image Representation*, vol. 31, pp. 208–224, 2015. 4
- [14] “Photomatix essential,” <http://www.hdrsoft.com>, Accessed: 2015-07-02. 4